The influence of particle type on the mechanics of sand-rubber mixtures.

R.Fu[+], M.R.Coop* and X.Q.Li[$]

R.Fu [+], PhD

Faculty of Engineering, China University of Geosciences, Wuhan, Hubei 430074, China

M.R.Coop *, PhD

University College London, formerly City University of Hong Kong

X.Q.Li[$] , PhD

College of Civil Engineering and Mechanics, Huazhong University of Science and Technology, Wuhan, Hubei 430074, China

Corresponding Author:

Matthew Richard, Coop

Department of Civil, Environmental and Geomatic Engineering

University College London

Gower street

London WC1E 6BT

U.K.

Tel: +44-7548896110

Email: mrcoop@cityu.edu.hk

ABSTRACT

Triaxial and oedometer tests were used to demonstrate that a critical state framework can be applied to sand-rubber mixtures of similar soil grain and rubber sizes. It was found to describe well the behavior of a crushable sand and a quartz sand with either rubber fibers or granules of a variety of quantities, from small to large strains. Together with additional oedometer tests on soils of a wider variety of gradings, the work enabled the influences of sand particle type, grading and rubber shape to be established. The sand particle type, specifically whether the grains were weak or strong, was found to be a key factor. It affected the yield in compression, even when large quantities of rubber were added. It controlled the critical state stress ratio, except for those mixtures with the highest content of rubber fibers, as well as the stress strain behavior. Sand particle type also determined the critical state line location in the volumetric plane for lower rubber contents, but at higher rubber contents the behavior tended to converge for the two sand types. The grading and rubber type were not found to affect the compression or swelling indices significantly, which were mainly controlled by rubber content. Gradings that had non-convergent compression paths without added rubber tended to retain this feature with rubber. The addition of both types of rubber led to higher volumetric compression in isotropic or one-dimensional compression but reduced volumetric strain during shear, altering the shapes of the state boundary surfaces.

Keywords: particle crushing/crushability; reinforced soils; residual soils; sands.

Introduction

Considerable research has been devoted to the behavior of rubber inclusions of various sizes in soils, generally in the form of shreds (50-305mm) or chips (12-50mm) but more recently also on smaller sizes. The aim has generally been to dispose of waste tire rubber whilst creating a lightweight fill with an enhanced strength. Table 1 gives a brief summary of the key previous research. The majority of studies focused on the monotonic behavior of sand-rubber mixtures, but in some, dynamic tests were performed and the data are included since dynamic and monotonic measurements of the elastic shear modulus should be closely related. Direct comparisons between the various data sets are generally not possible, the various papers having emphasized different aspects of behavior with materials and/or methods that are often not easily comparable. A very wide variety of rubber contents (RC) has also been used, either quantified by volumetric proportions or by weight. For ease of comparison they are all shown in–weight fractions, having converted the volumetric contents if necessary. Because individual parameters are not easily compared, the summary focusses on the principle conclusions reached and to what extent a critical state framework was used, which is the topic of this paper.

The improvement in strength has been variable, with shreds and larger chips often increasing peak strengths (e.g. Edil & Bosscher, 1994; Foose et al., 1996) especially for higher aspect ratios (Zornberg et al., 2004). In contrast, smaller chips, crumbs or granules more typically either have no effect on strength or a negative one (e.g. Masad et al., 1996; Youwai & Bergado, 2003; Kawata et al., 2007; Lee et al., 2007). At the smaller size, aspect ratio has proven to be important, and attention has more recently focused on rubber buffings, which are threads typically created by the tire re-treading process. In shear box tests Edinçiler & Ayhan (2010) found these to give a greater strength increase in sand than granules of rubber. However, for clays Ozkul & Baykal (2007) found that rubber fibers gave no strength benefit at higher stress levels. They attributed this to a need to have dilative volumetric strains to mobilize tension in the fibers to create a reinforcing effect.

Despite the very large amount of research work undertaken, there have been few attempts to place the behavior of soil-rubber mixtures within a critical state or steady state framework as might usually be done for other, more "standard" soils. The effects of confining pressure and/or density on various aspects of behavior have been investigated by a number of researchers (e.g. Foose et al., 1996; Zornberg et al., 2004; Mashiri et al., 2015), and Youwai, & Bergado (2003) fitted a critical state based model to their data. However, in Table 1 it is clear that the behavior is generally investigated in the shear stress: normal stress plane, or q':p' in terms of invariants, while little is shown in the volumetric plane v:lnp' (v specific volume, =1+e). An exception to this is the work by Tsoi & Lee (2011), who investigated a rubber, cement, fly ash and sand mixture. Although the sand content was very small, so the material is quite different to the sand-rubber mixtures studied here, the research is included in Table 1 because they specifically adopted a critical state framework, identifying similar critical state lines for cemented and uncemented mixtures.

There is no inherent reason why the behavior of rubber mixtures cannot be investigated in the v:lnp' plane. As Youwai & Bergado (2003) have pointed out, the bulk modulus of the rubber is high, which has two implications. Firstly the principle of effective stress is applicable (Yajima & Kobayashi, 2007), and secondly the specific volume is not significantly altered by the bulk compressibility of the rubber. Following the successful application of a critical state framework to polypropylene fiber reinforced sands by Santos et al. (2010), Fu et al. (2014) therefore applied a critical state framework to the behavior of mixtures of rubber fibers and granules in a completely decomposed granite (CDG), showing that unique critical state lines could be identified in the v:lnp' plane, just as for other soils. They also found that the strengthening effect of rubber fibers was not dependent on dilation but could also be seen in a compressive soil.

While Fu et al. (2014) established that critical states can be identified in sand-rubber mixtures, the investigation was limited to a local Hong Kong CDG and only at large strains. The current paper extends this work in various ways, 1) making comparisons with the same rubber added to a more standard quartz sand, so that the relative roles of the particle nature, rubber content and rubber shape could be determined, 2) making a more detailed investigation of the application of a critical state framework, including the identification of isotropic normal compression lines and state boundary surfaces, 3) the small strain behavior has been investigated, and 4) a detailed investigation was made of how the interaction of grading and rubber content controls the compression behavior. Some data from Fu et al. are repeated here, but that repetition has been kept to a minimum, including only those data needed for comparisons or to derive a more complete critical state framework.

The aim of this work was not to optimize rubber contents, sizes or shapes for particular soils, but to investigate the applicability of key soil mechanics concepts to rubber-sand mixtures. The choice of the two base soils, the CDG and a quartz sand, enables the effects of rubber to be contrasted in base soils that have weak and strong particles and that are predominantly compressive and dilative respectively. The investigation of mixtures of stiff soil grains with deformable rubber grains also has wider implications for our understanding of soils with mixed mineralogies.

Materials and Procedures

The main part of the research was carried out on two single sized sands, the Hong Kong CDG and the quartzitic Leighton Buzzard sand (LBS). Both were sieved to have the sizes of 0.6-1.18mm. While the LBS has stronger rounded and sub-rounded quartz particles and is typically dilative at engineering stress levels, the CDG has weaker sub-angular particles and is more compressive. The comparison of the two highlights the relative roles of particle and rubber characteristics in determining the overall behavior. Establishing the validity of a critical state framework for both ensures that it should be more generally applicable for sand-rubber mixtures. In addition, an extensive oedometer investigation of the factors controlling compression behavior was carried out using a wider range of gradings of the CDG. All the gradings tested are indicated in Fig.1.

The rubber added was either in the form of granules (GR) of the same size as the soil particles or rubber buffing fibers (RF), the comparison allowing the influence of aspect ratio to be separated from the effect of simply adding a quantity of rubber. The buffing fibers had a mean length 10.5mm and diameter 1.26mm, with a mean tensile breakage load of about 8.4N and mean breakage strain of 210%. The rubber contents (RC) used were generally 10% and 30% by dry weight, representing typical values investigated in the literature. The rubber was randomly mixed with the soils.

All of the oedometer and triaxial samples for the 0.6-1.18mm particle size presented in this paper were created by moist-tamping, using sufficient tamping to remove any macro-voids. Under compaction (Ladd, 1978) was used for the triaxial samples, tamping into the membrane held in a mold on the pedestal. The oedometer samples were compacted at as wide range of initial specific volumes as could be achieved. This wide range was necessary to check whether the compression curves for different densities would converge onto a unique normal compression line (NCL) or if “transitional” behavior could be observed with non-convergent compression paths (e.g. Altuhafi et al., 2010; Shipton & Coop, 2012). For the wider range of gradings tested only in the oedometer some samples were created by dry compaction or air pluviation to achieve a greater range of initial specific volumes, but no effect on the compression behavior arising from the preparation method could be detected.

The aim of this work was a fundamental investigation of the applicability of conventional soil mechanics frameworks rather than optimizing the density and/or rubber content for application. The triaxial samples were therefore mostly created at loose initial states with the intention to be able to reach the isotropic Normal Compression Line (NCL) and so examine if unique state boundary surfaces (SBS) could be identified. A variety of triaxial sample sizes were used, mostly using 75x150mm or 60x120mm, but with a few of the small strain tests at the 38x76mm size. Comparisons between local and global (i.e. with an external volume gauge) volume changes during isotropic compression showed that the volumetric strains were very similar. This means that there was no significant membrane penetration for the externally measured volume changes. No other effects of sample size could also be seen. A correction for membrane stiffness was made (Fukushima & Tatsuoka, 1984). Saturation under back pressure for the triaxial tests generally gave B values over 98% and always over 95%. All of the shearing was carried out drained. To measure the small strain behavior, some of the tests had local LVDTs (Cuccovillo & Coop, 1997) along with axially mounted bender elements. The bender elements were excited with a single shot sine wave and the velocity was interpreted from the first arrival, using techniques described by Jovicic et al. (1996).

The specific volumes were determined from 1) the initial dry unit weight, and 2) the final water content, using specific gravities of 2.58 for CDG, 2.65 for LBS and 1.15 for the rubber. After accounting for the recorded volumetric strains during testing, an average of the two values was taken and an estimate of the accuracy was made by taking half the difference. The mean value of this "accuracy" was about ±0.02, which is slightly greater than is typical for conventional soils (e.g. Rocchi & Coop, 2014) perhaps because sample preparation as well as the measurement of dimensions and weights was a little more difficult.

One-Dimensional Compression of Uniform Gradings (0.6-1.18mm).

The oedometer samples of the uniform sands were generally made at loose states with similar initial specific volumes. However, for the 10% rubber contents a range of initial specific volumes was made in order to check if for each soil the compression paths for different densities would converge to unique one-dimensional NCLs, or if there was any evidence of transitional behavior with compression paths that do not converge. Shipton & Coop (2012) had found that this type of behavior for soils with mixed mineralogy, so it was thought possible that it might occur for mixtures of such diverse particles as sand and rubber. No transitional behavior could be found and for each rubber content for the CDG there is a unique NCL on Fig.2. These NCLs move downwards as the rubber content is increased, as Fu et al. (2014) had highlighted from a more limited series of tests.

Yield of poorly graded sands is associated with the onset of particle breakage (e.g. Coop & Lee, 1993), and is at a much higher stress for the quartz particles of the 100% LBS than for the CDG. Even when rubber is added, the particle characteristics still control whether and when a NCL is reached, so that the CDG mixtures all reach their NCLs at fairly similar stress. For the LBS a stress of 7MPa is insufficient to bring the soil onto a unique straight NCL either without rubber or at 10% rubber content. For the 30% rubber fiber content the compression curves of the LBS only just approach an NCL at this stress. The addition of the rubber does, however, make the yield in compression less distinct in both soils, since there are larger volumetric strains during the initial stages of loading. As the rubber content increases the differences in compression behavior of the two sands are also reduced.

Fu et al. (2014) showed that the addition of rubber tended to reduce the particle breakage in the CDG, but these data are not repeated here. Figure 1 gives some gradings for the LBS after testing, confirming that in both the pure soil and the rubber mixtures, there was minimal particle breakage.

In unloading the effect of rubber inclusion was pronounced in both soils. There is a change from an almost rigid unloading for the pure sands to much more recoverable strains for the high rubber contents. The swelling lines for the rubber-sand mixtures had a distinct S-shape even when using a logarithmic stress scale. This means that the straight NCLs for the CDG mixtures must to some extent be coincidental, since they result from non-linear elastic and plastic components of compression.

It is tempting to believe that the greater compressibility of the rubber-soil mixtures might be related to a higher compressibility (i.e. low bulk modulus) of the rubber phase, but this is not the case because the bulk modulus of vulcanized rubber of 2.7GPa is actually higher than that of water (Hencky, 1932). The volume change of the rubber phase at the stress levels tested here is therefore not significant. The increased compressibility of the mixture must instead result from the very low shear modulus of the rubber (570kPa; Hencky, 1932), and it is its distortion not its compression that increases the global volume change. The effect of adding rubber is considerable and at high rubber contents the compression paths start to curve as they approach the limiting v=1 at high stress levels. This indicates that the distortion of the rubber, combined with substantial particle breakage in the case of the CDG, must be so severe that the void spaces are almost filled.

One-Dimensional Compression of Other Gradings.

To investigate further the influence of the base soil on the overall behavior, a more extensive series of oedometer tests was carried out on a wider variety of CDG-rubber mixtures. The CDG was chosen as the base soil for this study because the NCLs could be identified within the stresses that could be reached. The effects of adding rubber could then be easily compared by means of the compression and swelling indices, C_c and C_s. The specific volume at 100kPa, v_{100}, was chosen to quantify the vertical location of the NCL in preference to the usual practice of taking a projected intercept at 1kPa. This was done to reflect better the actual location of the NCL at the stresses for which it could be identified. An intercept that is projected can be misleading if there are significant variations in gradient. A variety of single gradings, gap gradings and well graded mixtures of CDG were tested with both the GR and RF, which are indicated in Fig.1. For the base soil the swelling lines were straight, while those when rubber was added tended to have the S-shape seen in Fig.2. For the mixtures, values of C_s were therefore chosen for the straighter part of the swelling curve after an initially stiffer stage, as in the example of Fig.3.

For the gap graded mixtures a transitional mode of behavior was observed, an example of which is given in Fig.4. Both the gap-graded base soil and the RF reinforced soil gave compression curves that did not converge, even at the highest stresses reached in the oedometer, tending to reach paths that were almost parallel. Ponzoni et al. (2014) quantified the degree of transitional behavior by plotting the void ratios at the highest stress reached in the oedometer against the initial values, the gradient of this relationship being defined as the parameter m. The values of m have been quantified here by using the void ratios at 3kPa and 3000kPa. No difference could be found between the GR and RF mixtures in the compression of the gap-graded CDG and they have not been distinguished in this analysis. The resulting m values are between 0.2-0.6 for all rubber contents (Fig.5) indicating a significantly non-convergent compression behavior. More generally, the gap-graded base soils that were transitional also gave transitional behavior when mixed with rubber. In contrast, the single graded or well graded base soils gave unique NCLs both with and without rubber, as in the examples of Fig.2.

Figure 6 summarizes all of the compression parameters for the various gradings of CDG, rubber contents and rubber types from over 100 tests. The data points have been highlighted according to the type of grading; single gradings have open points, gap graded solid and well graded crosses. The scatter of the data certainly hides some significant differences between samples with different gradings and rubber types. For example the finest single grading (0.15-0.30mm) tends to give lower C_c and C_s values than the coarser gradings. Nevertheless these summary plots do emphasize important general conclusions, and for both C_c and C_s the bands of data points are not large considering the wide variety of gradings and the two rubber types tested.

The C_c values (Fig.6a) do not change much up to a rubber content of about 30%, after which they steadily increase. For most gradings there is even a small drop in C_c from the pure soil to a 10% rubber content. At very high rubber contents the data for the single gradings tend to give lower values of C_c than the well graded or gap graded. The effect of adding rubber on the C_s values (Fig.6b) contrasts with the effect on C_c, with a rapid initial increase of C_s from RC=0-10% and then a slower rate of increase at higher RC. At larger rubber contents the rate of increase of C_s is slightly less than that for C_c. Again there is a tendency for lower C_s values for the single gradings than for the well graded or gap graded mixtures. For neither C_s nor C_c is there any clear effect of the rubber type on the compression parameters.

In Fig.6(c) the v_{100} data divide into two distinct bands, one for the single sized gradings (open symbols) and one that is much lower for the well graded (crosses). No data are shown for the gap graded samples because there is no unique value of v_{100} for these. Within each band there is no clear effect of the grading or rubber type. For both grading types v_{100} generally reduces as RC increases. There is some evidence that a minimum v_{100} is reached for the well graded samples as the 50% RC data points plot slightly higher than those at 30%. At the very high RC values the v_{100} values of the uniform and well graded samples converge.

Shearing

Stress-Strain Curves

Typical shearing data for the single sized (0.6-1.18mm) LBS and CDG are shown in Fig.7. These examples are for tests at an initial mean normal effective stress (p'_0) of 200kPa. To be able to compare the data for the two soils and the contributions of the rubber more easily, the stress ratio q'/p' has been normalized by the value of M for each base soil, M_s, which is 1.30 for LBS and 1.40 for CDG, reflecting the more angular nature of the CDG particles. These values were assessed over all the tests conducted and from both the stress-strain data and the stress-dilatancy graphs, so the two tests shown here on the 100% soils do not necessarily converge perfectly with a q'/M_sp' value of 1.0.

As will be discussed later, the loose initial preparation states meant that most of the samples were compressive during shearing. The CDG is generally less stiff than the LBS, and when 30% RF is added to the already softer response of the CDG the ultimate strength takes strains of over 40% to be mobilized. But in general the addition of rubber has a more noticeable effect on the stress-strain behavior and volume changes of the LBS than the CDG and the relatively modest effects of adding rubber on the stress-strain behavior and volume changes for the CDG are perhaps surprising, particularly for a volumetric content of 50%. As will be discussed later, the increase in ultimate strength is only significant for the 30% RF content in either soil.

Small Strain Stiffness

Bender element readings of the elastic shear modulus in the vertical plane G_{vh} were made on the pure sands and the 30% RF mixtures. A single shot sine wave was used and Fig.8 gives a typical set of received traces for a range of frequencies. The first arrival, T_a, was chosen from these plots, ensuring that there was consistency for the various frequencies used.

Examples of the Young's moduli are given in Fig.9. These have been calculated by taking tangents to short sections of the stress-strain curves, using similar techniques to Gasparre et al. (2014). For the rubber-soil mixtures the behavior was highly non-linear and no linear region of behavior could be detected even at smallest strain levels resolvable. Since the elastic values of the Young's moduli could not be found, the comparisons with the bender element data on Fig.10 are therefore only qualitative in nature. It is highly likely that anisotropy also affects the comparison, but the degree of anisotropy cannot be quantified with only vertical Young's moduli and G_{vh} data, and those for different strain levels.

There is generally a similar pattern of increase of stiffness with p' for the rubber-soil mixtures as for the pure soil. These may be approximated as straight lines on a log-log plot, as observed by Kim & Santamarina (2008, Table 1) for G_{vh}, but here the relationships are seen for a variety of strain levels. These lines tend to converge gradually for the LBS and LBS-rubber mixture, similar to the patterns observed for pure sands by, for example, Jovicic & Coop (1997). In contrast, they are almost parallel for the CDG and CDG-rubber mixture. The rubber has, however, a much greater effect on the intercepts of these lines than their gradients. The same features that were highlighted from the large strain data can also be seen here. The LBS is clearly much stiffer than the CDG, as expected from similar previous comparisons between CDGs and quartz sands (e.g. Jovicic & Coop, 1997). The effect on the stiffnesses of adding the rubber is then more pronounced for the LBS but the LBS remains considerably stiffer than the CDG even with 30% rubber content. Since a 30% weight content is equivalent to 50% by volume, it is again interesting to what extent the soil particle characteristics continue to influence behavior even in the presence of a very large quantity of rubber.

Critical States

The stress-strain and volumetric strain data indicate that there is a trend towards reasonably constant stresses and volumes for both soils, which have been assumed to be critical states. However, very large strains are needed to reach them. Figures 11 and 12 show the isotropic compression data, the drained shearing paths and the critical states. The CSLs for the CDG (Fig.11) have been slightly adjusted from those presented by Fu et al. (2014) in the light of additional data. The isotropic NCLs have also been added to Fig.11, which Fu et al. had not identified. It is a common assumption within critical state soil mechanics that the NCL and CSL are parallel. If they are not then a unique boundary surface cannot be determined using conventional techniques of normalizing for volume, as have been adopted here. Within some small data scatter this assumption seems to be supported. For the 100% CDG (Fig.7a) the stress levels reached may not have been quite sufficient to reach the isotropic NCL and so the chosen line is tentative, as indicated by the question mark.

As discussed above, the estimated errors of the values of v were on average about ±0.02 and it was not found possible to improve on this for these mixtures. The scatter of the data is consistent with this. Nevertheless, it is clear for the CDG (Fig.11) that as rubber is added both the NCL and CSL tend to move downwards. The separation of the NCL and CSL also reduces as rubber is added, especially for the GR, for which the separation for 30% content is so small that it cannot be resolved accurately within the small scatter of the data. An implication of the proximity of the NCL and CSL for the high rubber contents is that during drained constant σ'_r shearing the volumetric strains shown on Fig.7 are predominantly the result of the increase of p'.

For the LBS (Fig.12), the tests on the pure soil are slightly dilative and give a fairly flat CSL at these relatively low stress levels. It would need tests at very high stress levels to identify the steepening of the CSL in the particle breakage region, as was observed by Klotz & Coop (2002) for a finer LBS. As the rubber is added the CSL again moves downwards and in the case of the LBS it becomes significantly steeper.

For the LBS no attempt has been made to identify the isotropic NCLs, which have clearly not been reached. Even at a stress of 7MPa in the oedometer tests the one-dimensional NCLS could not be reached and larger stresses would normally be needed to reach an isotropic than a one-dimensional NCL. During isotropic compression the paths for the LBS-rubber mixtures seem almost to follow the CSLs and their divergence with them is slow, so an isotropic NCL could only be reached at very high stresses. Then during drained shearing the paths again remain close to the CSL. The fact that the isotropic compression and drained shearing paths are not more different reinforces what was seen for the CDG mixtures, that the volume change during shearing again arises predominantly from the increase of p ´not the change of q ´. This means that the relatively modest volume changes that occur during shearing are not a function of whether the sand is crushable or not and confirms that it is the rubber that causes this feature.

Figure 13 compares the CSLs for the various mixtures in the v:lnp' plane. The addition of rubber gives a greater effect on the location of the CSL for the dilative LBS than the compressive CDG, especially to its gradient. The greater effect on the location of the LBS CSLs means that at 30% RF or GR content the lines for the two soils are quite close. Nevertheless, these comparisons indicate that the location of the CSL in the v:lnp ´plane must be related more to the rubber content than to the nature of the soil particles. It is also clear that the type of rubber only has a secondary effect, because the CSLs for 10% GR and RF with CDG are the same and at 30% content both soils have CSLs in similar locations for GR and RF, but with slightly different gradients.

The critical state data are shown in the q':p' plane in Fig.14. The data have again been normalized by M_s to compare better the effects of the rubber in the two soils. The data points for the 100% sand samples should therefore plot on a line of gradient 1.0 (Fig.14a) and at lower stress levels they plot close to this. There is a little scatter in the data, mostly from slightly incomplete testing for the CDG at higher stress levels, causing the points to plot slightly low. For the LBS there was also a tendency for some tests for the q/p' to drift downwards at the end of the test, possibly as a result of some strain localization. The chosen M_s therefore reflect the values chosen over all stress levels and also took account of the stress-dilatancy plots that will be discussed later.

As discussed earlier, the least complete tests were those for the 70% CDG /30% RF. For correct comparison of the strengths at critical state, it is necessary that the comparison be made for constant stress states and using data from incomplete tests would lead to incorrect conclusions. Slight extrapolations of the critical state q/p ´were therefore made for the 70% CDG /30% RF mixture from the stress-dilatancy data that are discussed later. On Fig.14(a) the extent of these extrapolations can be seen to be small in most cases. After also normalizing for M_s, there is then very little difference between the CSLs for the 30% RF in LBS and CDG. This indicates that the effect of rubber in terms of ultimate strength is comparable in the two soils regardless of the nature of the soil grains. The CSL is curved and may be described by Eqn.1:

$$\frac{M_m}{M_s} = 5.4 \times 10^{-4} p' + 1.451 \qquad \text{Eqn.1}$$

where M_m is the value of q'/p' at critical state for the mixture. The effect of adding 30% RF is to reinforce the soil significantly, but curvature of the CSL means that there will be no effect at higher stress levels than those used here. For the 30% GR and both 10% GR and 10% RF there is no measurable reinforcing effect within the scatter of the data. It is interesting that relatively large amounts of rubber (up to 50% by volume) can be added without influencing significantly the value of M.

State Boundary Surfaces

The shearing data for each of the mixtures have been normalized for volume in an attempt to identify the state boundary surfaces (SBS) of each (Fig.15). The approach adopted has been to use an equivalent pressure taken on the CSL:

$$p'_{cs} = \exp\{(\Gamma - v)/\lambda\} \qquad \text{(Eqn. 2)}$$

Two methods have been used to reduce the scatter arising from small inaccuracies in the measurement of specific volume. For the CDG samples that have reached the isotropic NCL the value of specific volume at the start of shearing has been adjusted to be on the chosen NCL in Fig.11. For samples of both soils that had not been compressed to sufficiently high stresses to reach the NCL, the critical state point has been adjusted so that it lies perfectly on the chosen CSL. The latter approach had to be adopted for all of the LBS-rubber mixture samples. The q axis has been further normalized with respect to the critical state value of M, which is M_s for the base soils, 10% mixtures and 30% GR mixtures, but for the 30% RF mixtures the individual values of M_m from Eqn.1 have been used for each stress level. This normalization highlights differences in the SBS of each mixture that are not simply the result of the changing strength.

The resulting normalized stress paths allow state boundary surfaces to be tentatively identified on the wet side of the CSL for the CDG. As the quantity of rubber increases, the separation of the NCL and CSL becomes narrower and the SBS becomes steeper. Chandler (1985) had predicted that materials with easily deformable particles would have a SBS with the CSL to the left of the apex. While the 100% CDG does have this feature the addition of 30% deformable rubber particles actually causes it to disappear as the overall volume changes due to shear reduce. This steepening of the surface indicates that for a soil undergoing significant particle breakage, the volumetric compression during shear caused by the addition of rubber is actually less than the volumetric strain resulting from the breakage of the soil particles it has replaced.

For the 100% LBS the paths are all on the dry side of the CSL. For both the 10% and 30% rubber contents the samples at the highest stress levels have initial states directly below the CSL and the normalized paths rise to the CSL via an S-shaped path, indicating that although the overall volumetric strains due to shearing are small, there are compressive followed by dilative strains. No attempt has been made to define a SBS for the LBS mixtures.

Stress-dilatancy relationships

Figure 16 compares the stress-dilatancy relationships of the two base sands and the 30% RF mixtures for tests at 200kPa. The mobilized stress ratios have again been normalized by M_s

so that the effects of the fibers can be more easily distinguished. As discussed earlier, the 100% CDG tests tended to be a little incomplete and for the 100% LBS at the end of test the q/p' value drifted down slowly, possibly due to some strain localization. The 100% CDG is compressive throughout while the LBS is dilative at large strains. However, these differences are practically erased by the addition of the rubber and the relationships for the two 30% mixtures are similar. The data for both rubber mixtures again indicate that the additional strength arising from the fibers is mobilized at larger strains. The only difference is that because of the dilative behavior of the base soil, the LBS 30%RF mixtures reaches higher stress ratios at lower strains than the CDG 30%RF. The stress ratio of the latter is still increasing and the volume still compressing when the test was ended.

Conclusions

The oedometer and triaxial tests described in this paper have examined the behavior of two base soils with different particle strengths, CDG and LBS, mixed with various contents of rubber fibers and rubber granules of similar size to the soil particles. An extensive series of oedometer test then investigated in greater detail the effects of the grading of the CDG on the compression behavior. The key aim of this research was to investigate the applicability of a critical state framework to sand-rubber mixtures and Table 1 indicates that there has been no previous similar investigation. Fu et al. (2014) had identified that critical states could be identified for the CDG mixture and how these moved in the v:lnp' plane. Here a complete critical state framework has been derived from small to large strains for the various mixtures using a uniform CDG, including normal compression lines and state boundary surfaces. That framework was found, however, to break down for gap-graded samples.

For the quartz LBS some aspects of the framework could not be so fully established because very high pressures would be needed to reach the NCLs. Nevertheless the application of the critical state framework to two very different base soils allows a number of conclusions to be made about the fundamental mechanics of sand-rubber mixtures, showing how different aspects of behavior are influenced by the four key factors: soil particle nature, soil grading, rubber content and rubber type.

The soil particle type, specifically whether the base soil is an easily crushable one or not, determines when yield and a normal compression line can be reached in compression. Particle type also has an effect on the stress-strain and small strain stiffness behavior in shearing, since the LBS samples remained stiffer than the CDG even at 30% rubber content. It has, however, only a significant effect on the volumetric strain during shearing at low rubber contents. Similarly, particle type only affects significantly the critical state line location and gradient in the v:lnp' plane at lower rubber contents. The critical state line gradient in the q':p' plane, M, is mostly controlled by the particle type, even at high rubber contents, with a higher M for the more angular CDG. Only the addition of 30% rubber fibers gives a significantly altered strength, but the effect of the fibers is the same for the two soils when considered relative to the M of the base soil.

The influence of grading was only investigated for the CDG in one-dimensional compression, where it was found to control the location of the NCL (i.e. v_{100}) but to have less impact on the NCL and swelling line gradients.

Rubber content was the dominant factor controlling both C_c and C_s, and so the ratio of elastic to plastic strains in compression. Most of the references in Table 1 have emphasized the increased compressibility and softer shearing behavior caused by the addition of various forms of rubber, but this work is the first comprehensive investigation of those effects in the v:lnp´ plane applying a critical state framework. Rubber content influenced strongly the stress-strain behavior in shear at all strain levels and it was the main factor influencing the volumetric strains during shear and so the stress-dilatancy relationship, the spacing of the

NCL and CSL and so the shape of the state boundary surfaces. The close spacing of these lines at high rubber contents means that the volumetric strains in these mixtures are dominated by the changes in p' and are much less affected by shear.

The type of rubber added (fibers or granules) had only smaller effects on the compression behavior and its main effects were on the stress-strain behavior during shear. In particular, the rubber type had an influence on the volume changes during shear, which in turn affect the spacing between the NCL and CSL in the v:lnp´plane and so the size of the state boundary surface. The strength was also influenced by the rubber type, because the rubber fibers gave a reinforcing effect when added in large quantities while the granules did not. This influence of aspect ratio of the effectiveness of rubber inclusions has commonly been observed (Table 1; Youwai & Bergado, 2003; Bergado et al., 2005; Zornberg et al., 2004; Edincliler & Ayhan, 2010), but this is the first investigation that has been able to identify the relative effects of particle type and rubber type on critical state strength.

Acknowledgements

The authors are grateful for the contributions of the following to the test program: Wang Wan-ying, Zhao Jing, Ren yi-nan, Leung Ching-lim. The work described in this paper was partially supported by a grant from the Research Grants Council of the Hong Kong Special Administrative Region, China (Project No. CityU 112813).

References

Altuhafi, F., Baudet, B.A. & Sammonds, P. (2010) The mechanics of subglacial sediment: an example of new "transitional" behaviour. Canadian Geotechnical J., 47(7), 775-790.

Anastasiadis, A., Senetakis, K. & Pitilakis, K. (2012) Small strain shear modulus and damping ratio of sand/rubber and gravel/rubber mixtures. J. Geotch. & Geolog. Eng., 30(2), 263-382.

Bergado, D.T., Youwai, S. & Rittirong, A. (2005) Strength and deformation characteristics of flat and cubical tyre chip-sand mixtures. Géotechnique, 55(8), 603-606.

Chandler, H.W. (1985) A plasticity theory without Drucker's postulate suitable for granular materials. J. Mechs. & Phys. Of Solids, 33, 215-226.

Coop, M.R. & Lee, I.K. (1993) The behaviour of granular soils at elevated stresses. Predictive soil mechanics, Thomas Telford, London, 186-198.

Cuccovillo, T. & Coop, M.R. (1997) The Measurement of Local Axial Strains in Triaxial Tests Using LVDTs. Géotechnique, 47(1), 167-171.

Edil, T.B. & Bosscher, P.J. (1994) Engineering properties of tire chips and soil mixtures. Geotech. Testing J., 17(4), 453-464.

Edinçliler, A. & Ayhan, V. (2010) Influence of tire fiber inclusions on shear strength of sand. Geosynthetics International. 17(4), 183-192.

Edinçliler, A., Baykal, G. & Saygili, A. (2010) Influence of different processing techniques on the mechanical properties of used tires in embankments. Waste Management, 30, 1073-1080.

Foose, G.J., Benson, C.H. & Bosscher, P.J. (1996) Sand reinforced with shredded waste tires. J. Geotech Engng., 122(9), 760-767.

Fu.R., Coop, M.R. & Li, X.Q. (2014) The Mechanics of a Compressive Sand Mixed with Tyre Rubber. Géotechnique Letters, 4, 238-243.

Fukushima, S. & Tatsuoka, F. (1984). Strength and deformation characteristics of saturated sand at extremely low pressure. Soils & Foundations, 24(4), 30-48.

Gasparre, A., Hight, D.W., Coop, M.R. & Jardine, R.J. (2014) The laboratory measurement and interpretation of the small strain stiffness of stiff clays. Géotechnique, 64(12), 942-953.

Hencky, H. (1932) The elastic behavior of vulcanized rubber. Proc. National Mechanics Meeting of Am. Soc. Mech. Eng., New Haven Conn., 217-222.

Jovicic, V. & Coop, M.R. (1997) The stiffness of coarse grained soils at small strains Géotechnique, 47(3), 545-561.

Jovicic, V., Coop, M.R. & Simic, M. (1996) Objective Criteria for Determining Gmax from Bender Element Tests. Géotechnique, 46(2), 357-362.

Kawata, S., Hyodo, M., Orense, R.P., Yamada, S. & Hazarika, H. (2007) Undrained and drained shear behavior of sand and tire chips composite material. Proc. Int. Workshop Scrap Tire Derived Geomaterials – Opportunities and Challenges, Yokosuka, Japan, Hazarika & Yasuhara (eds), 277-283.

Kim H-K. & Santamarina J.C. (2008) Sand-rubber mixtures (large rubber chips), Can. Geotech. J., 45(10), 1457-1466.

Klotz, E.U. & Coop, M.R. (2002) On the Identification of Critical State Lines for Sands, Am. Soc. Test. Materials, Geotechnical Testing J., 25(3), 289-302.

Ladd, R.S. (1978) Preparing test specimens using undercompaction. Geotech. Testing J., 1(1), 16-23.

Lee, C., Shin, H. & Lee, J-S. (2014) Behavior of sand-rubber particle mixtures: experimental observations and numerical simulations. Int. J. Numer. Anal. Meth. Geomech., 38, 1651-1663.

Lee, C., Truong, Q.H., Lee, W. & Lee, J-S. (2010) Characteristics of rubber-sand particle mixtures according to size ratio. J. Materials in Civil Eng., 22(4), 323-331.

Lee, J-S, Dodds, J. & Santamarina, J.C. (2007) Behavior of rigid-soft particle mixes. J. Materials in Civil Engng, 19(2), 179-184.

Masad, E., Taha, R., Ho, C. & Papagiannakis, T. (1996) Engineering properties of tire/soil mixtures as a lightweight fill material. Geotech. Testing J., 19(3), 297-304.

Mashiri, R.F., Vinod, J.S., Neaz Sheikh, M. & Tsang, H-H. (2015) Shear strength and dilatancy behaviour of sand-tyre chip mixtures. Soils and Foundations, In Press.

Ozkul, Z. H., and Baykal, G. (2007). Shear behavior of compacted rubber fiber-clay composite in drained and undrained loading. J. Geotech.. Geoenviron. Engng., 133(7), 767-781.

Ponzoni, E., Nocilla, A., Coop, M.R & Colleselli, F. (2014) On the Identification and Quantification of Transitional Modes of Behaviour in the Sediments of the Venice Lagoon. Géotechnique, 64(9), 694 -708.

Rocchi, I. & Coop, M.R. (2014) Experimental accuracy of the initial specific volume. Geotech. Testing J., 37(1), 169–175.

Santos, A.P.S., Consoli, N.C. & Baudet, B.A. (2010) The mechanics of fibre-reinforced sand. Géotechnique, 60(10), 791-799.

Senetakis, K. & Anastasiadis, A. (2015) Effects of state of test sample, specimen geometry and sample preparation on dynamic properties of rubber-sand mixtures. Geosynthetics Intnl, 22(4), 301-310.

Shipton, B. & Coop, M.R. (2012) On the compression behaviour of reconstituted soils. Soils and Foundations, 52(4), 668-681.

Tsoi, W.Y. & Lee, K.M. (2011) Mechanical properties of cemented scrap rubber tyre chips. Géotechnique, 61(2), 133-141.

Valdes, J.R. & Evans, T. M. (2008) Sand-rubber mixtures: Experiments and numerical simulations. Can. Geotech. J., 45(4), 588-595.

Yajima, J. & Kobayashi, N. (2007) Isotropic pressure loop test and constant effective stress test on used tire rubber chips. Proc. Int. Workshop Scrap Tire Derived Geomaterials – Opportunities and Challenges, Yokosuka, Japan, Hazarika & Yasuhara (eds), 253-260.

Youwai, S. & Bergado, D.T. (2003) Strength and deformation characteristics of shredded rubber tire – sand mixtures. Can. Geotech. J., 40, 254-264.

Zornberg, J.G., Cabral, A.R. & Viratjandr, C. (2004) Behaviour of tire shred – sand mixtures. Can. Geotech. J., 41, 227-241.

Nomenclature

B	Skempton pore pressure parameter ($=\Delta u/\Delta\sigma_r$)
C_c	compression index
C_s	swelling index
CDG	completely decomposed granite
CSL	critical state line
$E_{0.01\%}$	tangent Young's modulus (subscript denotes axial strain level)
G_{vh}	elastic shear modulus in vertical plane
GR	granular rubber
LBS	Leighton Buzzard sand
M	critical state line gradient (q'/p')
M_m	value of M for 30% RF mixtures
M_s	value of M for base soil
NCL	normal compression line
p'	mean normal effective stress $= (\sigma'_a + 2\sigma'_r)/3$
q'	deviatoric stress $= \sigma'_a - \sigma'_r$
RC	rubber content
RF	rubber fibers
T_a	first arrival time for bender element tests
u	pore pressure
v	specific volume
v_{100}	specific volume intercept at 100kPa on one-dimensional NCL

ε_a	axial strain
ε_v	volumetric strain
σ'_a	axial effective stress
σ'_r	radial effective stress
σ'_v	vertical effective stress

Table 1. A summary of previous research on the monotonic behavior of sand-rubber mixtures

Reference	Soil Grading	Soil Type	Rubber Size	Rubber Content RC	Apparatus/ Tests	Principal Conclusions	Application Critical State Framework
Edil & Bosscher (1994)	Sand	Quartz	Chips, mean width 53mm	0-0.25	Shear box Proctor mold as oedometer	Shear strength increased above that of dense sand for RC >0.1. Large initial plastic displacements for mixtures in compression.	Data not examined in v:log stress plane
Foose et al. (1996)	Uniform DS_{50} =0.58mm	NS	Shreds, length <50-150mm	1 & 0-0.16	Shear box	Peak strength increases as RC increases & as density increases.	Data not examined in v:log stress plane
Masad et al. (1996)	Uniform DS_{50} = 0.23	Quartz, sub-rounded	RS_{50}=3.2mm	0, 0.3 & 1	Triaxial	Peak strength reduced & ε_v during shearing becomes more compressive as RC increases.	Data not examined in v:log stress plane
Youwai & Bergado (2003) & Bergado et al. (2005)	Poorly graded DS_{50} = 0.5mm	NS	RS_{50}=7mm cubical & RS_{50} = 13.7mm flat	0-1	Triaxial	As RC decreases, compression index reduces & ε_v during shearing becomes more dilative. Cubical rubber decreased strength for all RC, flat increased strength at lower RC. Flat chips increased compressibility more than cubical. Sand dominated behavior for RC>0.3.	State parameter controls stress-strain behavior but data not presented in v:log stress plane
Zornberg et al. (2004)	Uniform DS_{50} = 0.4mm	Quartz, rounded /sub-rounded	Chips width 12.7 or 25.4mm, AR = 1-8.	0-1	Triaxial	ε_a at peak strength increases with RC. Apart from high RC samples, soil dilative with peak strength at stresses applied. Optimum peak strength for RC=35% & peak increases with AR. Greater increase of strength at lower stresses. Relative density has less effect on strength for mixtures	Data not examined in v:log stress plane Critical states not analyzed & some tests did not reach critical states.
Lee et al. (2007) & Kim & Santamarina (2008)	Uniform DS_{50} = 0.35	Quartz, sub-rounded	RS_{50} =0.09 & 3.5mm	0-1	Oedometer with bender elements. Triaxial.	For DR_{50} =0.09mm sand dominated for RC<0.23 & for intermediate RC rubber dominated at low stresses & sand at high. Peak strengths reduced by rubber. For DR_{50} = 3.5mm sand dominated for RC<0.16 rubber dominated for RC>0.4 with no stress dependency for intermediate RC. G_{vh} and constrained modulus power functions of stress. G_{vh} higher for RC=0.05-0.1than at RC=0.	Data not examined in v:log stress plane & critical states often not reached.
Valdes & Evans (2008)	Uniform DS_{50} = 0.73	Quartz, rounded	RS_{50} =1.3mm	1 & 0.4	Oedometer & isotropic compression	Large hysteresis loops for load-unload. Larger residual strains in oedometer than iso comp. Smaller difference between iso comp and 1D for RC=0.4	Data not examined in v:log stress plane
Lee et al. (2010)	Uniform D_{50} = 0.725mm	Quartz, angular	RS_{50} =0.256-3.375mm	0-1	Oedometer with bender elements	Compressibility increases & G_{vh} decreases as RC increases & rubber size reduces. Transition from rubber like to sand like behavior at RC=0.23-0.4	Data not examined in v:log stress plane

Edincliler et al. (2010)	Sand	NS	RS=1-3mm	0-1	Shear box	Strength increased for all RC except RC=1	No volume change measurements & data not examined in v:log stress plane
Edincliler & Ayhan (2010)	Sand	NS	Crumbs & buffings RS=1-3mm AR=1 Thickness 3mm AR=3 Thickness 4.5mm AR=7	0-1	Shear box	For AR=1 peak strength generally decreased by rubber. Strength increased for larger AR up to an optimum at RC=0.2 for AR=7, then strength decreases with further RC increase.	No volume change measurements & data not examined in v:log stress plane
Tsoi & Lee (2011)	Sand	NS	Chips RS_{50} =10mm Bonded with Portland cement and fly ash	Ratio 1 chips :0.35 cement :0.2 4 ash :0.06 sand	Triaxial	Behavior similar to other cemented soils but with greater ductility.	Linear critical state lines identified in q:p' & v:lnp' plane, similar for bonded soil & same constituents but unbonded.
Anastasiadis et al. (2012) & Senetakis & Anastasiadis (2015)	Poorly graded DS_{50} = 0.27-7.8mm	Quartz	RS=0.35-3.0mm	0-0.35	Resonant Column	Addition of rubber reduced G_0 but had a similar effect to considering the rubber as void space. DS_{50} to DR_{50} ratio affects G_0.	No strength data
Lee et al. (2014)	Uniform DS_{50} = 0.73mm	Quartz, angular	Granules RS_{50}= 0.73mm	0-1	Oedometer with bender elements, resonant column & shear box.	Change from sand to rubber dominated from RC=0.23-0.4 Elastic range of behavior increases as RC increases. Higher exponent for G_{vh} with p ´for higher RC.	Critical state friction angle reduces as RC increases. Data not examined in v:log stress plane
Fu et al. (2014)	Uniform DS=0.6-1.18mm	Decomposed granite, sub-angular	Granules RS=0.6-1.18mm & buffings	0, 0.1 & 0.3.	Oedometer & triaxial	Strength can be increased by 30% buffings even if soil is compressive not dilative. 10% contents and 30% granules did not affect strength.	Critical state lines can be identified in both q:p ´and v:lnp ´ planes.

DS diameter soil particles, NS not specified, RS rubber size, AR aspect ratio, RC rubber content by weight

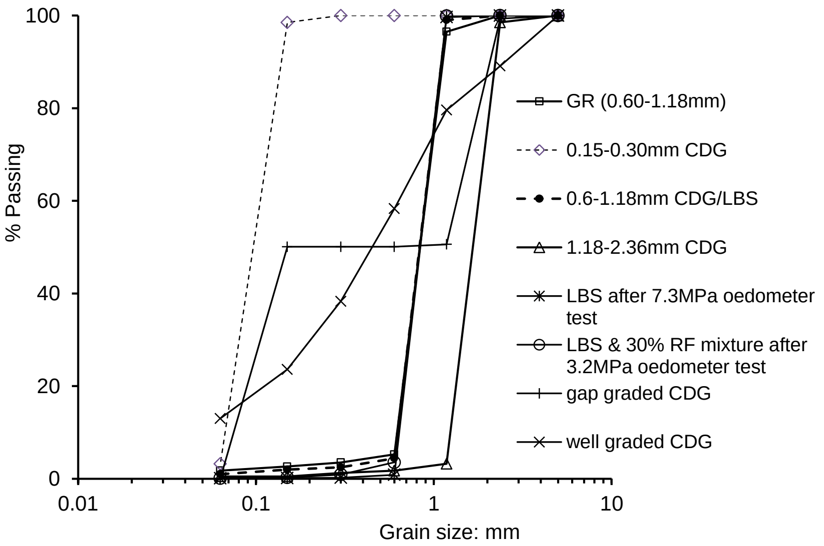

Fig.1 Gradings of soils used and measurements of breakage for the LBS mixtures.

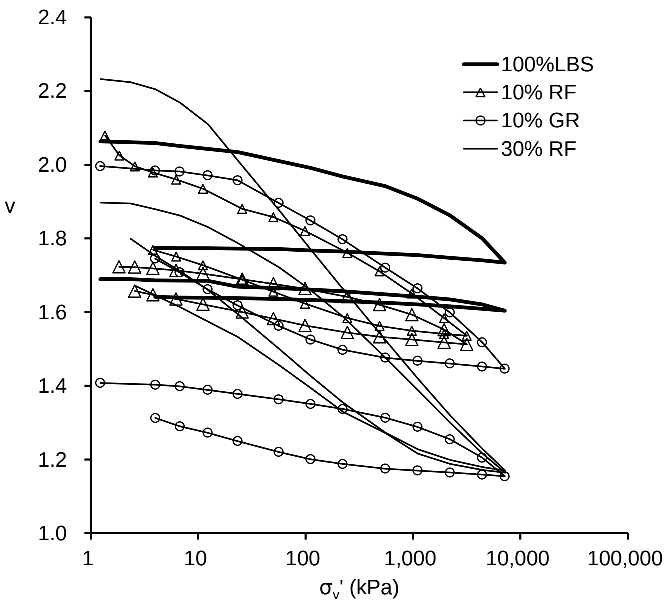

(a) Leighton Buzzard sand

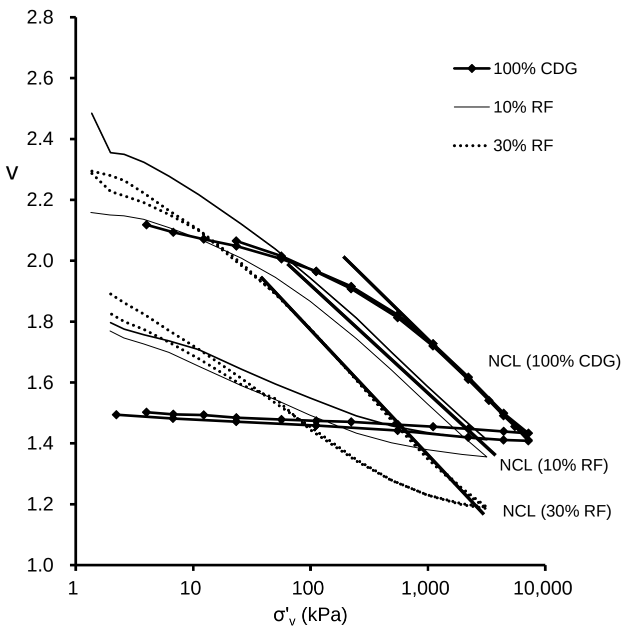

(b) CDG with rubber **fibers**

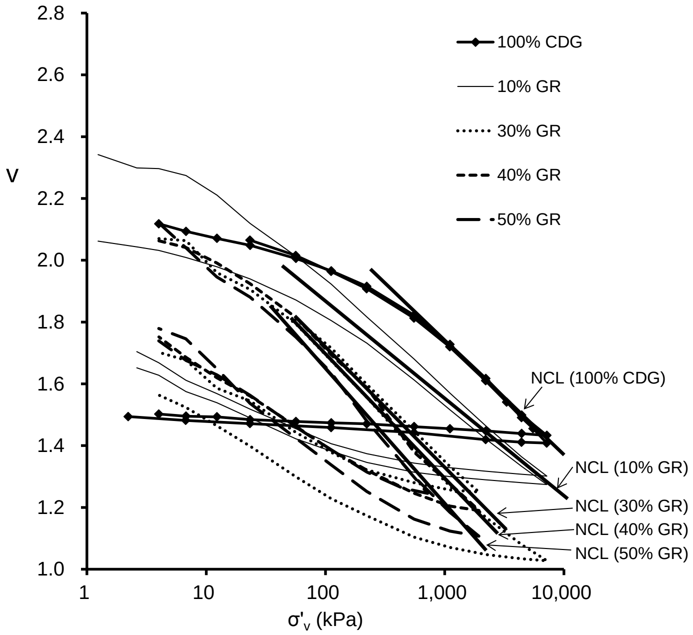

(c) CDG with rubber granules

Fig.2 Oedometer compression data (b and c modified from Fu et al., 2014)

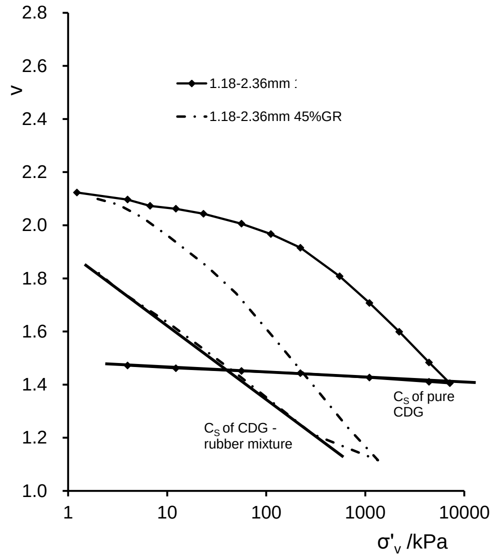

Fig.3 Examples of the selection of the swelling indices.

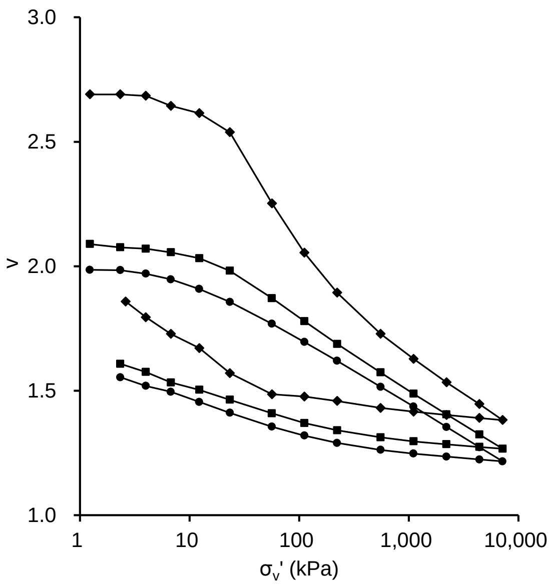

Fig.4 An example of non-convergent or “transitional” behavior for oedometer tests on a gap graded CDG with 10% GR.

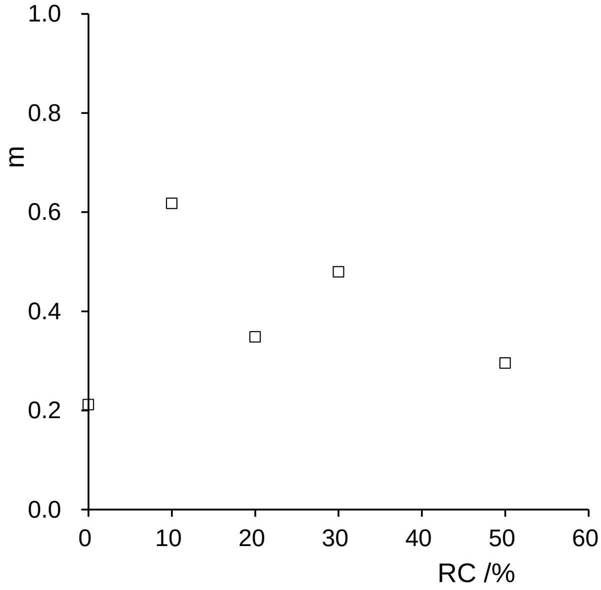

Fig.5 Values of m for the gap graded transitional mixtures.

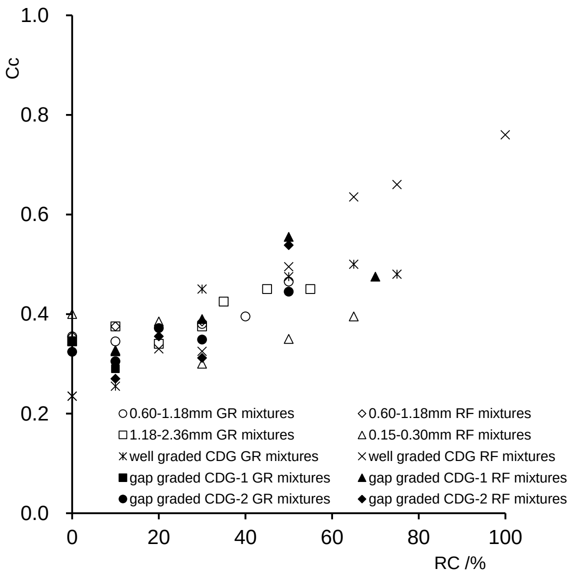

(a) Compression indices

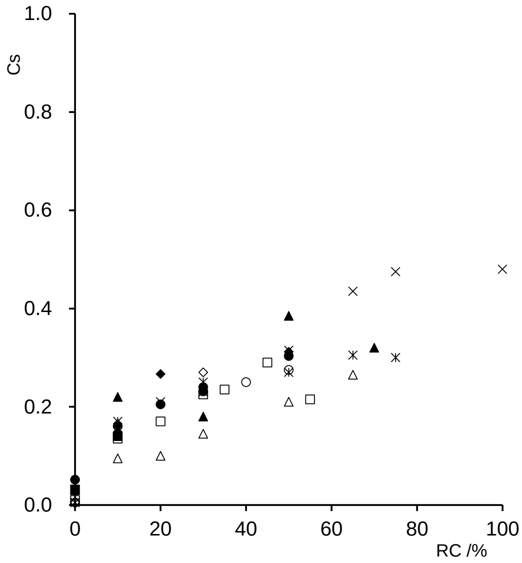

(b) Swelling indices

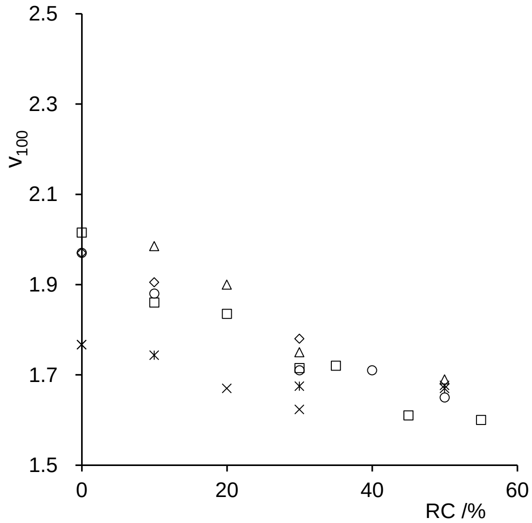

(c) Intercepts on one-dimensional NCL at σ'_v= 100kPa (single graded and well graded samples only)

Fig.6 Variation of oedometer compression parameters with CDG grading, rubber type and rubber content (open points: single gradings, solid points: gap graded, crosses: well graded).

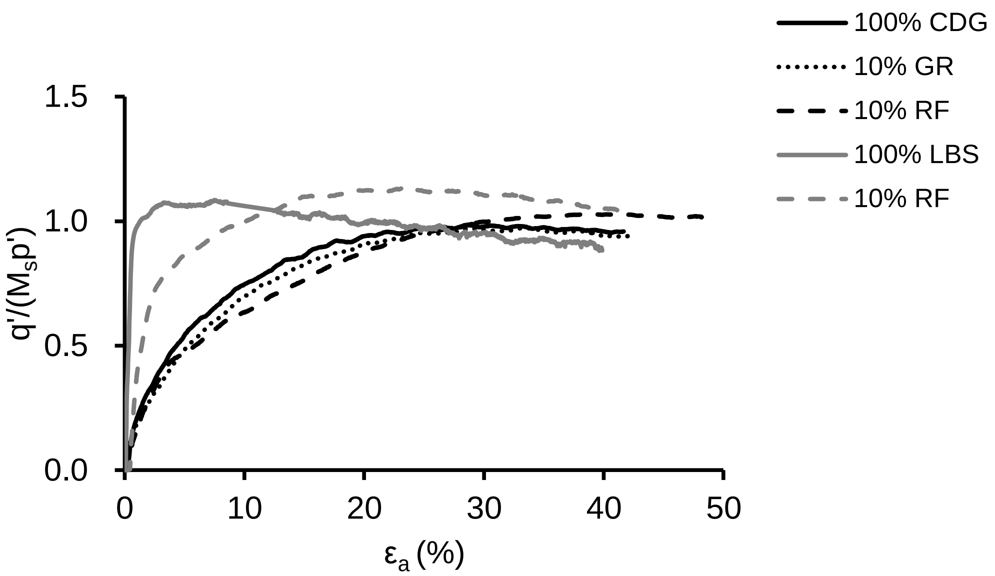

(a) stress-strain curves 10% rubber content

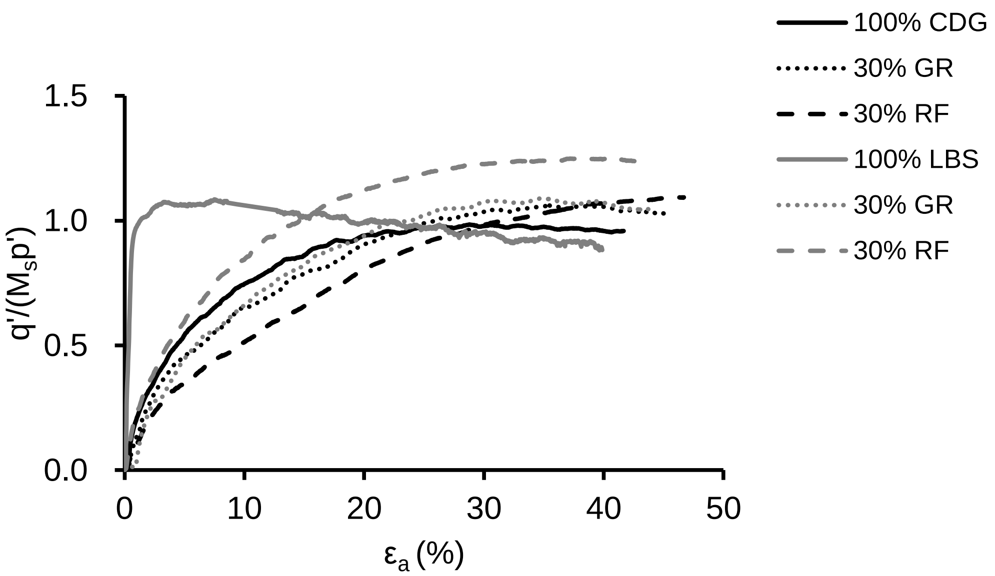

(b) stress-strain curves 30% rubber content

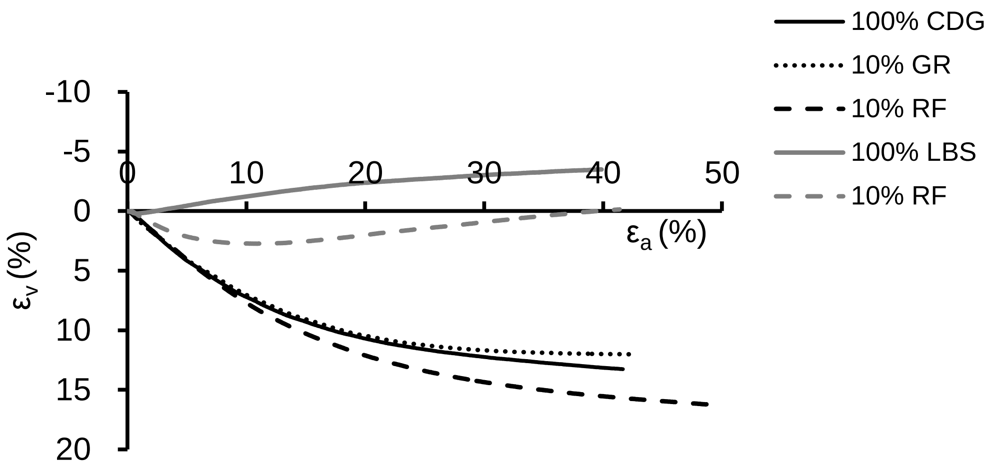

(c) volumetric change 10% rubber content

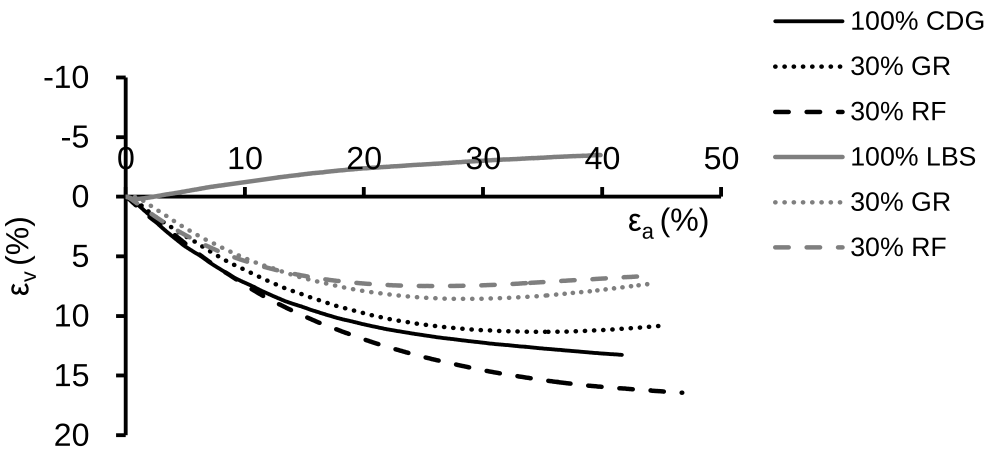

(d) volumetric change 30% rubber content

Fig.7 Examples of the stress-strain behavior of sand and rubber-sand mixtures at p'_0=200kPa.

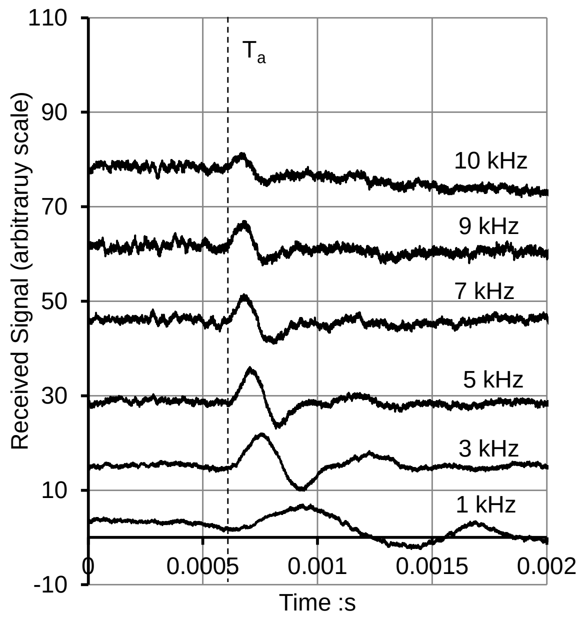

Fig.8 Typical bender element traces (70% CDG 30% RF at p'=400kPa)

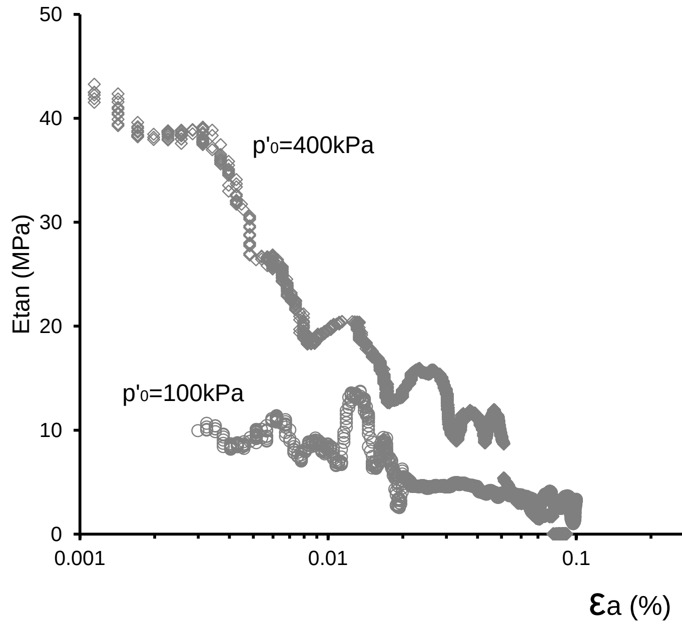

Fig.9 Typical stiffness decay curves for 70% CDG 30% RF.

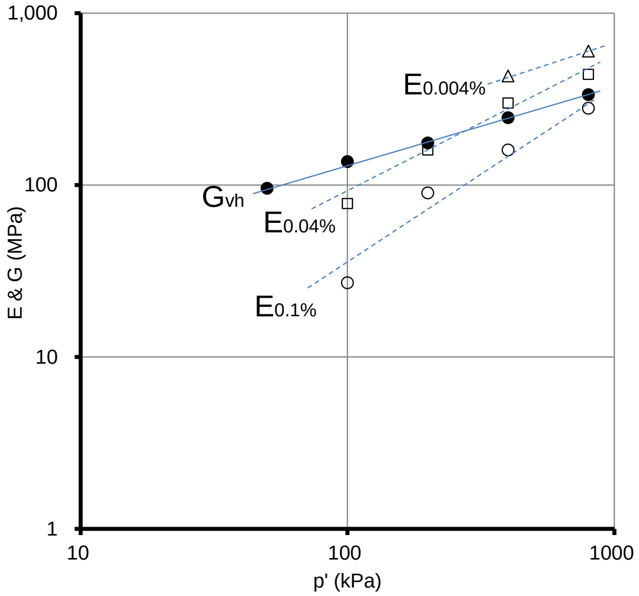

(a) 100% LBS

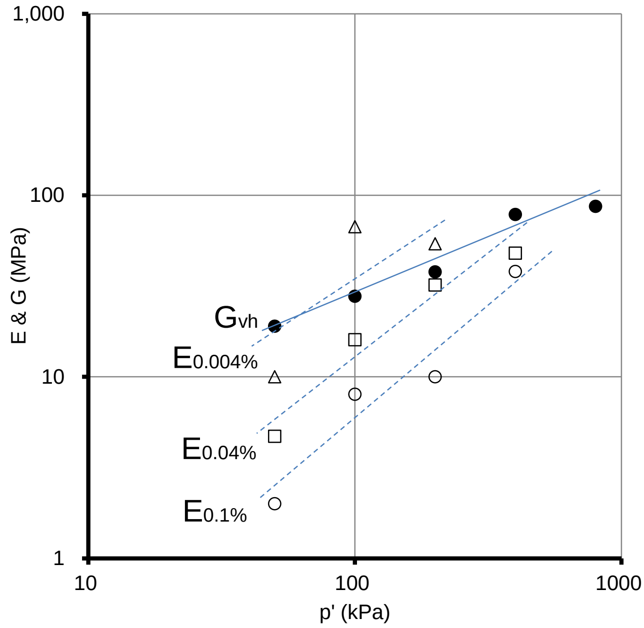

(b) 70% LBS 30% RF

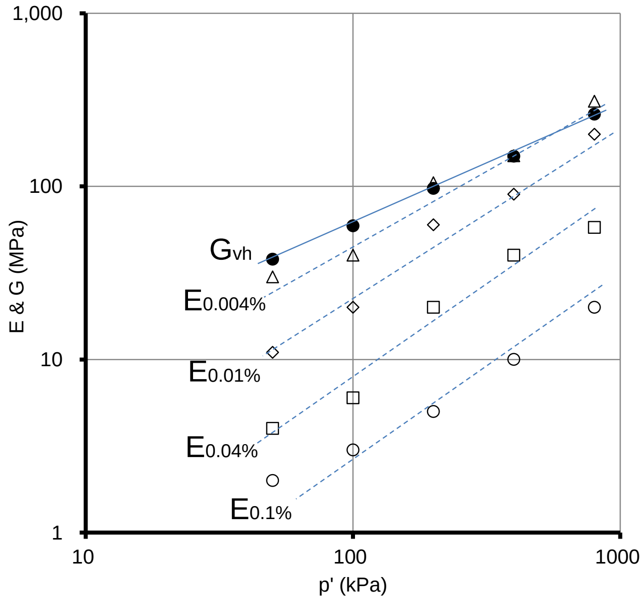

(c) 100% CDG

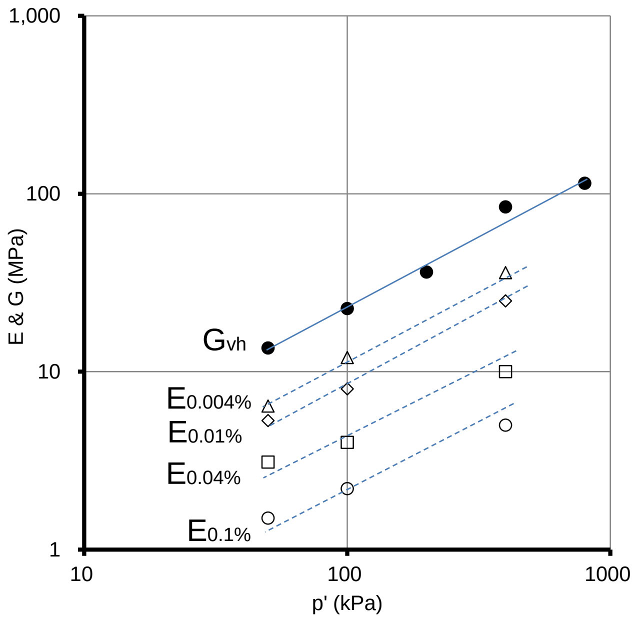

(d) 70% CGD 30% RF

Fig.10 Small strain stiffness of pure sands and rubber-sand mixtures

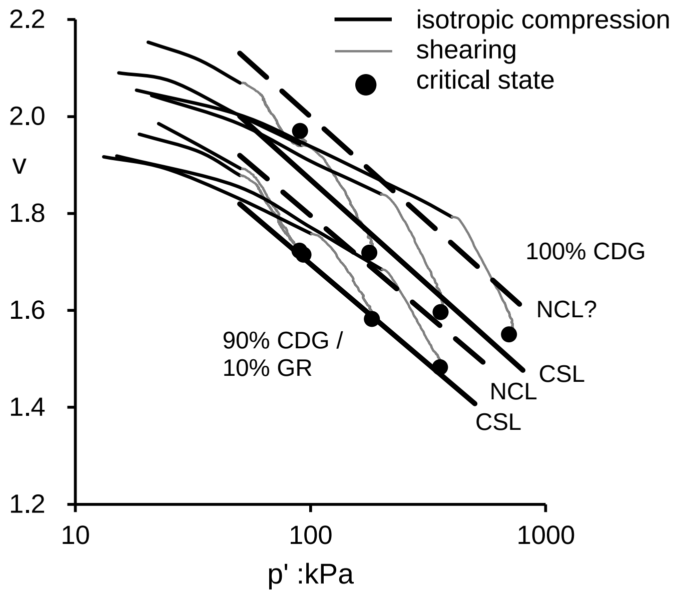

(a) 100% CDG and 90% CDG/10% GR (NCL? tentative location of NCL)

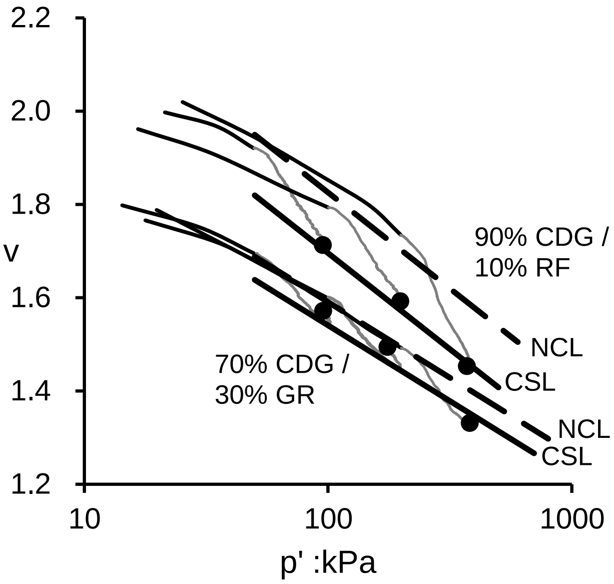

(b) 90% CDG/10% RF and 70% CDG/30% GR

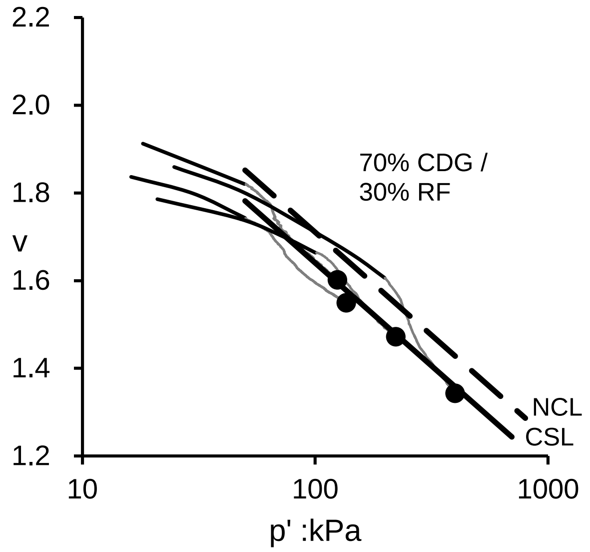

(c) 70% CDG/30% RF

Fig.11 Normal compression lines and critical state lines for CDG mixtures.

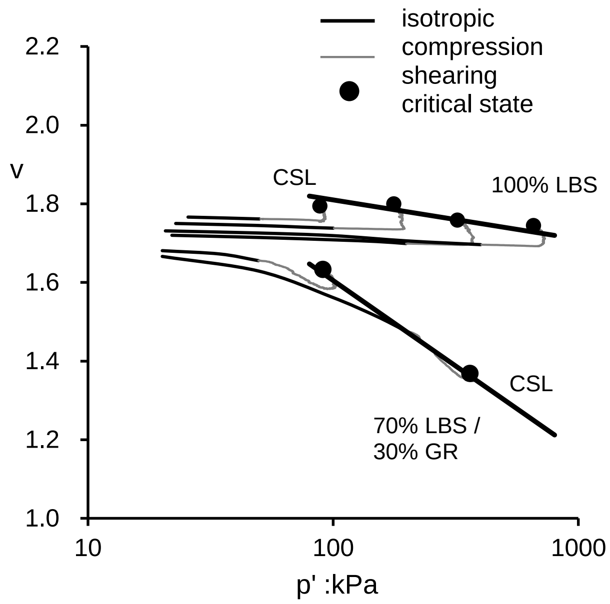

(a) 100% LBS and 70% LBS/30% GR

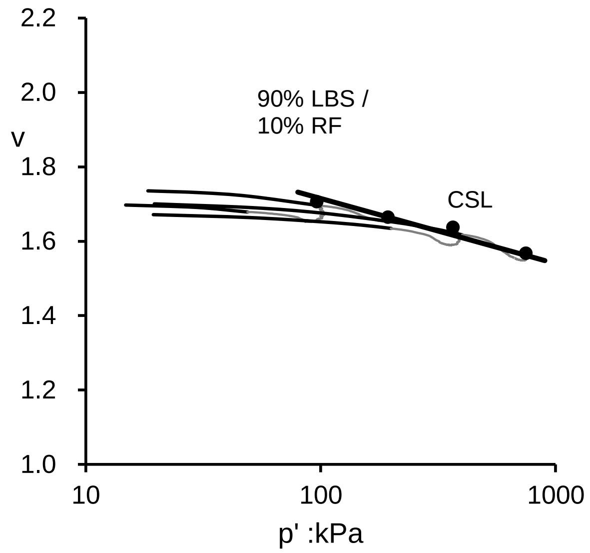

(b) 90% LBS/10% RF

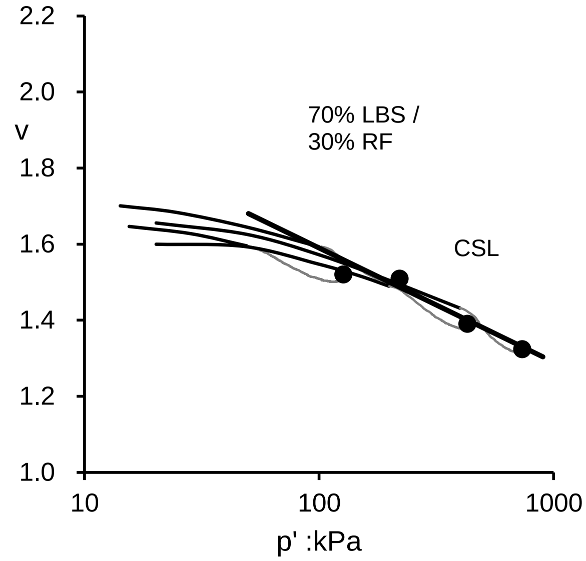

(c) 70% LBS/30% RF

Fig.12 Critical state lines for LBS mixtures.

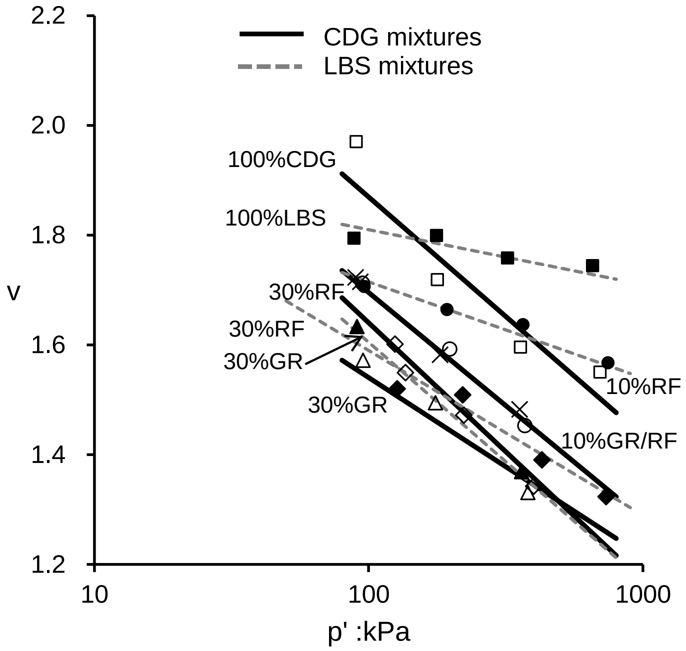

Fig.13 Comparison of critical state lines for LBS and CDG in the v:lnp' plane (open symbols CDG, closed symbols LBS).

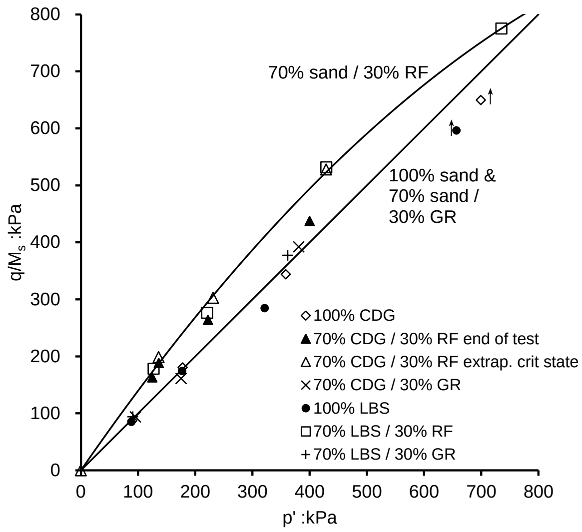

(a) 100% sand and 70% sand / 30% rubber mixtures

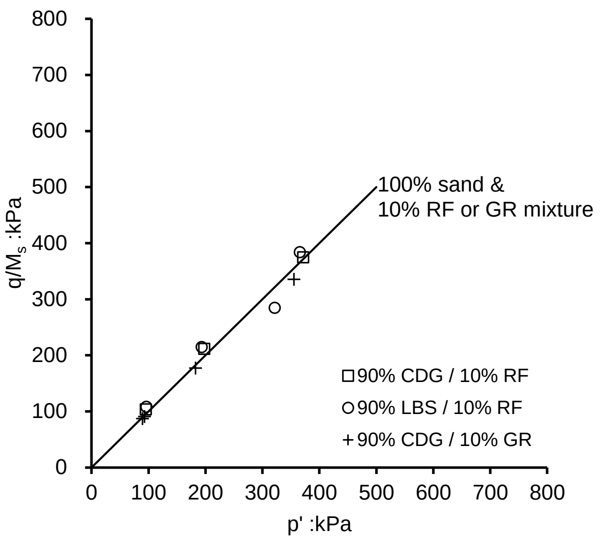

(b) 90% sand / 10% rubber mixtures

Fig.14 Comparison of critical state lines for the various mixtures.

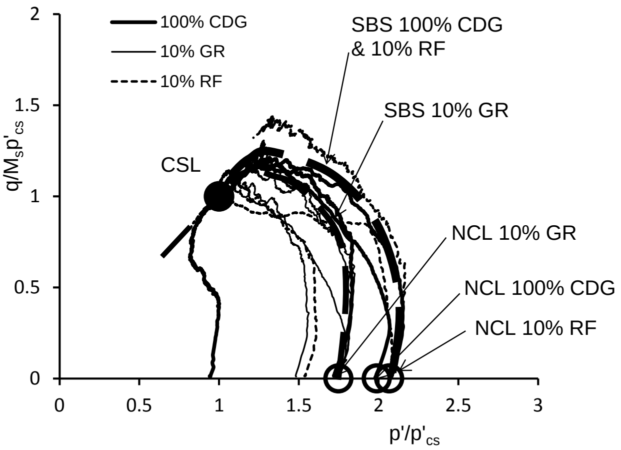

(a) 100% CDG and 10% mixtures

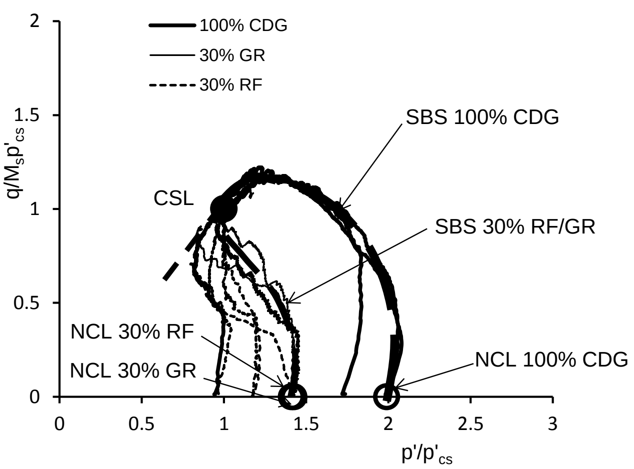

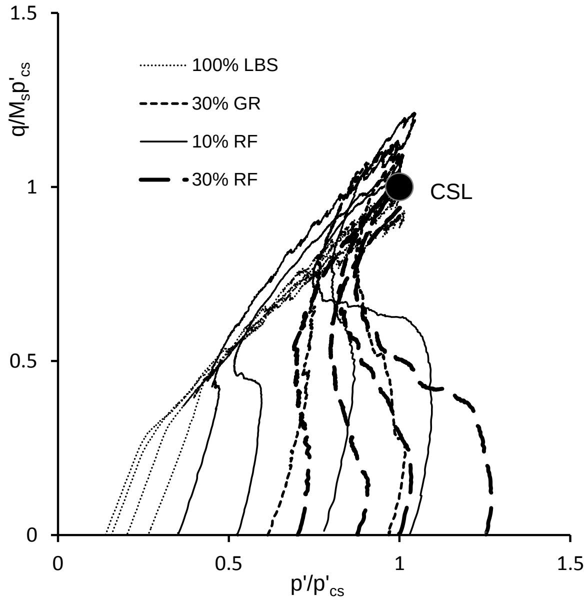

(b) 100% CDG and 30% mixtures

(c) LBS mixtures

Fig.15 Normalized stress paths and state boundary surfaces

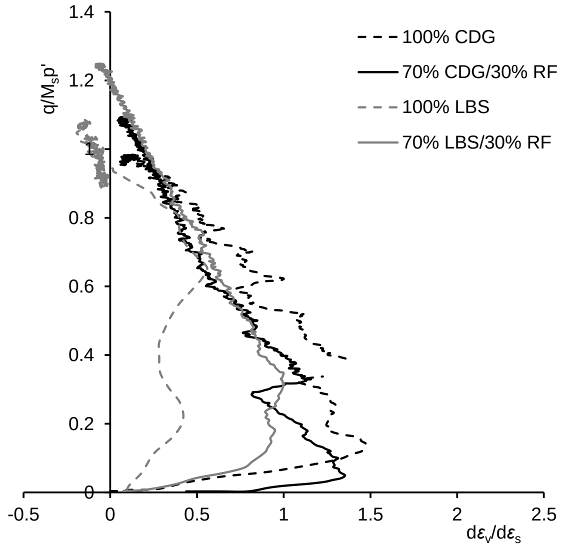

Fig.16 Stress-dilatancy data at p'_0=200kPa for pure sands and 30% RF mixtures.